



## The crystal structure of arginyl-tRNA synthetase from *Homo sapiens*



Hyun Sook Kim, So Young Cha, Chang Hwa Jo, Ahreum Han, Kwang Yeon Hwang\*

Division of Biotechnology, College of Life Sciences and Biotechnology, Korea University, Seoul, Republic of Korea

### ARTICLE INFO

#### Article history:

Received 23 April 2014

Revised 12 May 2014

Accepted 12 May 2014

Available online 22 May 2014

Edited by Michael Ibba

#### Keywords:

Arginyl-tRNA synthetase

L-Canavanine

L-Arginine

Rossmann fold

tRNA<sup>Arg</sup>

Enzyme Commission number (6.1.1.19)

### ABSTRACT

**Arginyl-tRNA synthetase (ArgRS) is a tRNA-binding protein that catalyzes the esterification of L-arginine to its cognate tRNA. L-Canavanine, a structural analog of L-arginine, has recently been studied as an anticancer agent. Here, we determined the crystal structures of the apo, L-arginine-complexed, and L-canavanine-complexed forms of the cytoplasmic free isoform of human ArgRS (hArgRS). Similar interactions were formed upon binding to L-canavanine or L-arginine, but the interaction between Tyr312 and the oxygen of the oxyguanidino group was a little bit different. Detailed conformational changes that occur upon substrate binding were explained. The hArgRS structure was also compared with previously reported homologue structures. The results presented here may provide a basis for the design of new anticancer drugs, such as L-canavanine analogs.**

© 2014 Federation of European Biochemical Societies. Published by Elsevier B.V. All rights reserved.

### 1. Introduction

Aminoacyl-tRNA synthetases (aaRSs) catalyze the esterification of amino acids to their cognate tRNAs during protein synthesis [1]. In the two-step reaction, aminoacyl adenylate formation occurs in the presence of amino acids, ATP and Mg<sup>2+</sup>, and then the aminoacyl group of the enzyme-bound intermediate is transferred to the 3'-end of the cognate tRNA to form an aminoacyl-tRNA [2]. The 20 aaRSs are divided into two groups based on characteristic conserved structural regions in their active site [2]; class I aaRSs contain 'HIGH' and 'KMSKS' motifs in the Rossmann fold, whereas class II aaRSs have three homolog motifs in the catalytic domain [2].

The class I arginyl-tRNA synthetase (ArgRS) localizes to the cytoplasm. In contrast to that of other organisms, mammalian cytoplasmic ArgRS exists as two isoforms that are generated from different translational initiations of the same mRNA. Two isoforms of ArgRS participate in protein synthesis and the N-end rule pathway of protein degradation with similar catalytic characteristics, respectively [3–9]. Like glutamyl- and glutaminyl-tRNA synthetases,

they also require the presence of cognate tRNA for amino acid activation [4,10–12]. During protein translation, one ArgRS isoform, a component of the multi-synthetase complex, interacts with several proteins, such as the tRNA-associating factor p43 and leucyl-tRNA synthetase, through its 72 amino acid N-terminal extension [6,13–15]. The second isoform, which lacks the N-terminal extension and exists as a free protein [5], is thought to play a role in the N-end rule pathway of ubiquitin-dependent protein degradation by participating in the formation and provision of Arg-tRNA<sup>Arg</sup> to arginyl-tRNA transferase for arginylation of all acidic N-terminal residue, as well as oxidized cysteine [3,4,7,16]. L-Canavanine, which was originally isolated from jack bean plant (*Canavalia ensiformis*), is an ArgRS substrate that can be incorporated as a structural analog of L-arginine [17,18]. L-Canavanine has an oxyguanidino group, in which the methylene group of arginine is replaced with an oxygen atom; hence, L-canavanine is slightly longer and less basic than L-arginine [19]. Recently, L-canavanine has been investigated as an anticancer agent because it is toxic to cancer cells and is particularly effective against the growth of pancreatic cancer cells [19,20]. Binding of L-canavanine into ArgRS may lead to the synthesis of proteins with abnormal functions or defective structures [21], and the disruption of protein degradation by the N-end rule pathway [3,7,19]. Determination of the structure of the ArgRS–L-canavanine complex would shed light on the mechanism by which this substrate is recognized.

Here, we determined the crystal structures of the free isoform of *Homo sapiens* ArgRS (hArgRS), including the apo form and the

**Abbreviations:** aaRS, aminoacyl-tRNA synthetase; hArgRS, free isoform of human ArgRS; PBD, Protein Data Bank; Nd, N-terminal domain; Ins1, insertion domain 1; Ins2, insertion domain 2; Cd, C-terminal domain; RMSD, root mean square deviation

\* Corresponding author. Address: Division of Biotechnology, College of Life Sciences and Biotechnology, Korea University, Seoul 136-701, Republic of Korea. Fax: +82 2 923 3229.

E-mail address: [chahong@korea.ac.kr](mailto:chahong@korea.ac.kr) (K.Y. Hwang).

complexes containing L-canavanine and L-arginine. Structural analyses confirmed that L-canavanine can be incorporated into the active site of hArgRS in place of L-arginine. The mechanism of L-canavanine recognition and orientation in the active site, and the interactions of residues in hArgRS with L-canavanine and L-arginine, are discussed. The conformational changes that occur upon binding to the substrate are also explained. Furthermore, based on structural superimpositions onto reported structures, the predicted interactions of each domain of hArgRS with tRNA<sup>Arg</sup> are discussed.

## 2. Materials and methods

### 2.1. Protein expression and purification

The gene encoding the cytoplasmic form of ArgRS lacking the 72 amino acid N-terminal region was amplified from *H. sapiens* genomic DNA by polymerase chain reaction and cloned into the pET28a vector (Novagen) at the *NheI* and *NotI* sites. The recombinant pET28a plasmid was transformed into *Escherichia coli* Rosetta (DE3) cells (Novagen), which were grown at 37 °C in Luria broth containing 100 µg/ml kanamycin until they reached an OD<sub>600</sub> of 0.6. Overexpression of hArgRS was induced by incubation with 1 mM isopropyl-β-D-1-thiogalactopyranoside at 18 °C for 16 h. The cells were harvested by centrifugation at 4000×g for 25 min, resuspended in buffer A (30 mM Tris-HCl, pH 8.0, and 150 mM NaCl) containing 1 mM phenylmethylsulfonyl fluoride, and then disrupted by sonication. The supernatant was obtained by centrifugation at 25000×g for 45 min, loaded onto a HiTrap™ column (GE Healthcare), and then washed with buffer A containing 20 mM imidazole. The hArgRS protein was eluted using the linear gradient method with buffer A containing 20–500 mM imidazole. After dialysis of the eluted protein against buffer B (30 mM Tris-HCl, pH 8.0), the protein was loaded onto a HiTrap™ Q HP column (GE Healthcare), which had been equilibrated with buffer B, and then eluted with a linear gradient of 0–1 M NaCl. Finally, the eluted protein was applied to a HiLoad 26/60 Superdex™ 200 column (Amersham), which had been equilibrated with buffer C (30 mM Tris-HCl, pH 8.0, and 100 mM NaCl). The highly purified protein (>95%) was obtained about 7.5 mg from a 4-L cell culture using *E. coli* expression and then concentrated to about 25 mg/ml for crystallization.

### 2.2. Crystallization and structure determination

Initial screening for hArgRS was performed with a screening kit for crystallization (Hampton Research). Single crystals were obtained using the hanging drop vapor diffusion method by mixing 1 µl of the protein with 1 µl of reservoir solution (0.085 M sodium citrate tribasic dehydrate (pH 5.7), 24% polyethylene glycol 4000, 0.17 M ammonium acetate, and 15% glycerol) for 2–3 days at 22 °C. To obtain the crystals complexed with L-arginine or L-canavanine, purified hArgRS was incubated for 2 h on ice with 1 mM L-arginine (Sigma) or L-canavanine (Sigma), respectively. The crystals were frozen in liquid nitrogen and X-ray diffraction data were collected using beamline BL1A at the Photon Factory, Japan. The data were integrated and scaled using the HKL2000 package [22]. The structure of *Saccharomyces cerevisiae* ArgRS (Protein Data Bank (PDB) entry: 1BS2) was modified using the PHENIX program sculptor [23] followed by a search model for molecular replacement with AutoMR. The structures of the apo and substrate-bound hArgRS complexes were refined with PHENIX [23] and manually built using the COOT application [24]. The refined structures that were validated by the MOLPROBITY program [25] are summarized in Table 1. The crystallographic data for apo, L-arginine complexed,

**Table 1**  
Data collection, phasing, and refinement statistics.

	Apo	L-Arginine	L-Canavanine
<b>Data collection</b>			
Wavelength (Å)	0.9800	0.9794	0.9870
Space group	P212121	P212121	P212121
Cell dimensions			
a, b, c (Å)	77.62, 105.23, 172.25	74.49, 106.90, 175.25	75.39, 109.31, 175.01
Resolution (Å) <sup>a</sup>	50.00–2.80 (2.85–2.80)	50.00–2.40 (2.44–2.40)	30–2.80 (2.85–2.80)
Reflections (Total/ Unique)	194070/33971	263322/55170	190567/ 35623
Redundancy	5.7 (3.4)	4.8 (3.2)	5.3 (3.4)
Completeness (%)	95.5 (89.1)	97.8 (95.4)	97.8 (95.7)
I/σ (I)	19.51 (3.78)	27.5 (3.04)	17.11 (2.85)
R <sub>merge</sub>	0.086 (0.314)	0.075 (0.306)	0.103 (0.313)
<b>Refinement</b>			
Resolution (Å)	45–2.8	40–2.4	30–2.8
No. reflections	33922	55082	35509
R <sub>work</sub> /R <sub>free</sub> (%)	20.81/26.78	19.62/25.37	20.51/26.23
No. atoms			
(Protein/Water/ Ligand/Glycerol)	9162/171	9478/275/24/ 28	9349/205/24
Average B factors			
(Protein/Water/ Ligand/Glycerol (Å <sup>2</sup> ))	47.50/36.01	47.50/46.4/ 43.32/48.34	42.00/32.12/ 21.14
<b>RMSD</b>			
Bonds (Å)	0.010	0.009	0.009
Angles (°)	1.384	1.111	1.219
<b>Ramachandran plot (%)</b>			
Favored regions	90.09	95.56	90.47
Allowed regions	8.66	3.67	8.74
Outlier regions	1.25	0.77	0.79

<sup>a</sup> The resolution range at the outer shell is shown in parenthesis.

and L-canavanine complexed hArgRS have been deposited in the PDB under IDs 4Q2Y, 4Q2T, and 4Q2X, respectively.

## 3. Results and discussion

### 3.1. Overall structure of hArgRS

The crystal structures of the apo, L-arginine complexed, and L-canavanine complexed forms of the free isoform of hArgRS were determined. Each crystal belonged to space group P2<sub>1</sub>2<sub>1</sub>2<sub>1</sub> and contained two molecules in the asymmetric unit. Analysis of the hArgRS crystals using the program PISA [26] showed that the surface of the dimer was 1153.2 Å<sup>2</sup>, and the gel filtration showed hArgRS exists as a monomer in solution, which suggests the dimer was induced by crystal packing. Analysis of the crystal structures revealed that hArgRS comprises five domains: an N-terminal domain (Nd) that includes residues 1–119; a catalytic domain, insertion domains 1 (Ins1) and 2 (Ins2) that are located at the N- and C-terminal ends of the catalytic domain, respectively; and a C-terminal domain (Cd) that includes residues 383–588 (Fig. 1A). The Nd, which is organized into four α-helices and an anti-parallel β-sheet containing four strands, is linked to the catalytic domain by a long loop. The catalytic domain is composed of two assembly regions and forms the Rossmann fold. The first region includes residues 230–260 and 120–170, and harbors the 'HIGH' motif (His136, Val137, Gly138, and His139). The second region includes residues 312–382. Ins1 comprises three α-helices and is located between the separated parts of the first region of the catalytic domain, while Ins2 contains a three-stranded anti-parallel β-sheet and connects the second region of the catalytic domain to the Cd. The Cd, which includes a bundle of eight α-helices (α13–α20), is situated next to

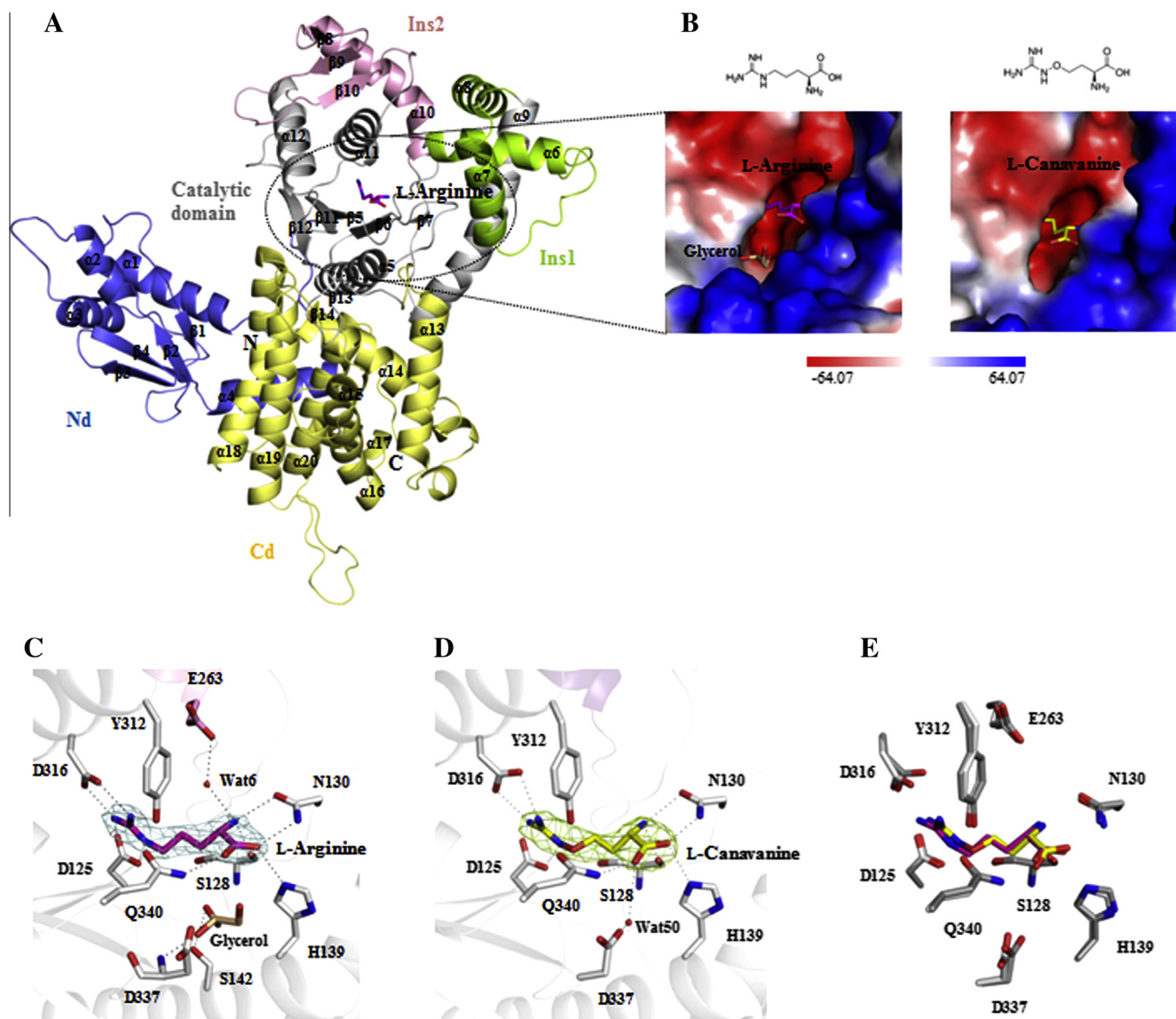


**Fig. 1.** (A) The overall structure of the cytoplasmic free form of *hArgRS* bound to *L*-arginine. The Nd, catalytic domain, Ins1, Ins2, and Cd are shown in blue, gray, green, pink, and yellow, respectively. *L*-Arginine is shown in magenta. (B) Magnified views of the substrates in the active site pocket are shown as electrostatic surface models. *L*-Arginine, glycerol, and *L*-canavanine are shown as magenta, wheat, and yellow stick models, respectively. The chemical structures of *L*-arginine and *L*-canavanine are shown above the images. (C, D) Magnified views of the binding sites in *hArgRS* for *L*-arginine and glycerol (C), and *L*-canavanine (D). *L*-Arginine, glycerol, and *L*-canavanine are colored as described for (B). The residues interacting with the substrates are depicted by stick models and the water molecules are shown as red spheres. Hydrogen bonds are indicated by black dotted lines. The omit map calculated around *L*-arginine and *L*-canavanine (shown in cyan and yellow, respectively) represents  $2.0 \sigma$ . (E) Superimposition of the interactions in the binding sites for *L*-arginine and *L*-canavanine in *hArgRS*. *L*-Arginine and *L*-canavanine are colored as described for (B). Interactions between *hArgRS* and *L*-arginine or *L*-canavanine are indicated as gray or dark gray stick models, respectively.

the Nd and the  $\alpha 18$  helix of the Cd interacts with the  $\beta 2$  strand of the Nd (Fig. 1A).

### 3.2. The *L*-canavanine recognition site

To confirm that *L*-canavanine can be incorporated into *hArgRS* in place of *L*-arginine, we determined the structure of the *hArgRS*-*L*-canavanine complex with 2.8 Å resolution. *L*-Canavanine bound to the solvent-accessible active site of *hArgRS*, which is organized by the C-terminal region of the Rossmann fold (Fig. 1B). The structural analysis revealed that *L*-canavanine is orientated with the oxyguanidino moiety docked inside the negatively charged pocket, and the carboxyl and amino groups of the substrate are positioned at the entrance of the active site pocket

(Fig. 1B). The residues preceding the  $\alpha 5$  and  $\alpha 11$  helices and the  $\beta 5$  strand participate in substrate recognition (Fig. 1A). The oxyguanidino moiety of *L*-canavanine forms a hydrogen bond with Tyr312 and salt bridges with the carboxylates of Asp125 and Asp316 (Fig. 1D). The carboxyl group of the substrate forms hydrogen bonds with the side chains of Asn130, Gln340, and His139. In addition, the nitrogen atom of the substrate's amino group is hydrogen-bonded to the side chain of Asn130 and the main chain of Ser128, and indirectly to the carboxylate of Asp337 via a water molecule. The oxygen of the substrate's oxyguanidino group forms a hydrogen bond with Tyr312. With the exception of Asp125, which is replaced with glutamate, these residues are conserved among different organisms (*S. cerevisiae*, *Pyrococcus horikoshii*, and *Thermus thermophilus*) (Fig. 4). In addition to Tyr312, two

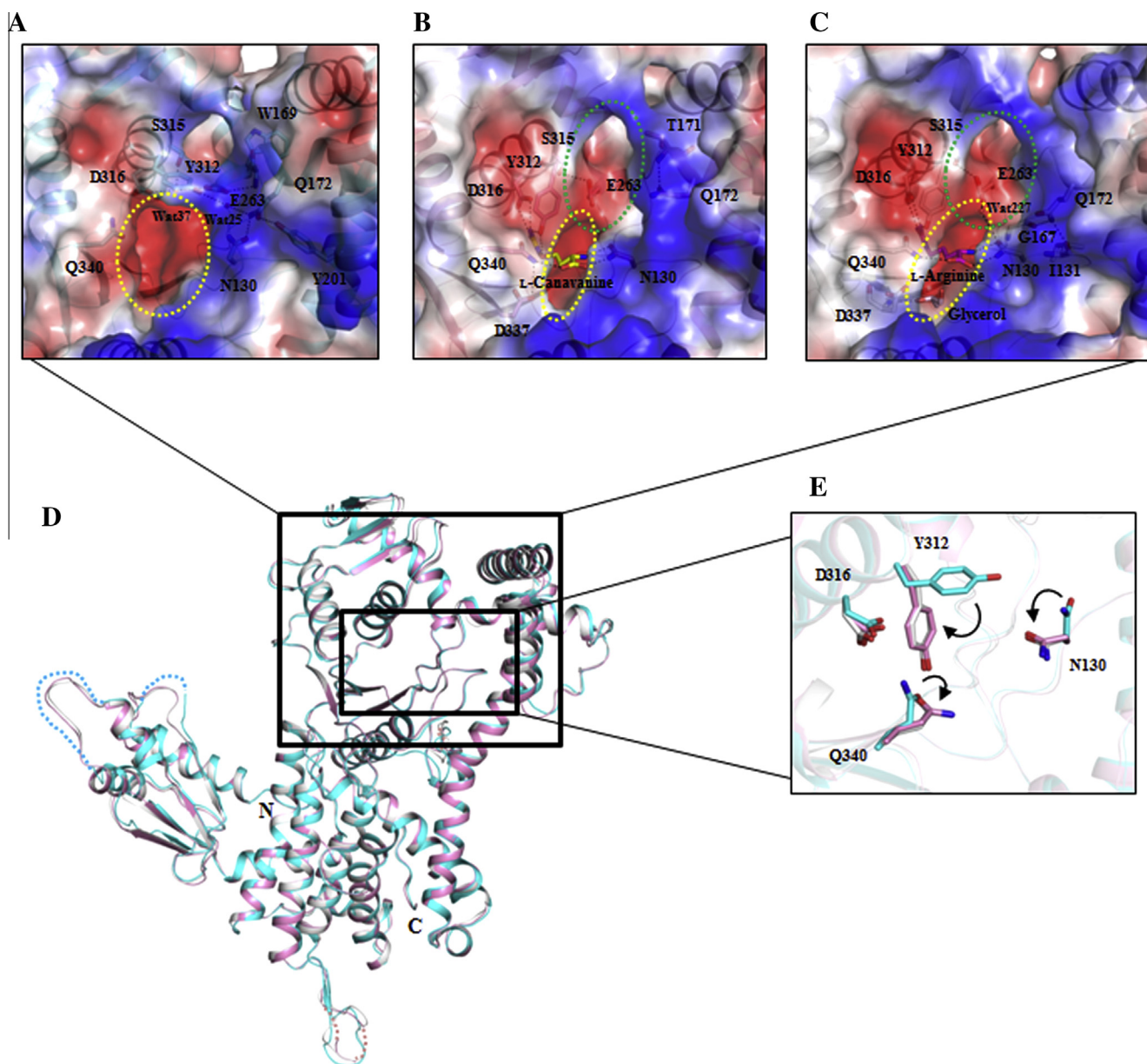


**Fig. 2.** (A–C) Structural comparisons of the apo (A), L-canavanine-complexed (B), and L-arginine-complexed (C) forms of *hArgRS* shown as electrostatic surface models. The residues that form hydrogen bonds are indicated by stick models and water molecules are shown as red spheres. Hydrogen bonds are indicated by black dotted lines. The active site pocket for the substrate and the cavity for binding of the tRNA<sup>Arg</sup> acceptor arm are represented by yellow and green dotted circles, respectively. (D) A structural superimposition of the apo (cyan), L-canavanine-complexed (pink), and L-arginine-complexed (gray) forms of *hArgRS*. Each structure is shown as a ribbon model. The large and small boxed areas, which are markedly different regions, indicate those shown in (A–C) and (E), respectively. The disordered regions are indicated by dotted lines. (E) Comparisons of residues in the active sites. The shifted residues are shown as stick models, which are colored as in (D). The directions of their shift are indicated by arrows.

negatively charged residues, Asp125 and Asp316, play essential roles in substrate distinction.

### 3.3. The L-arginine recognition site

Next, we determined the structure of the *hArgRS*-L-arginine complex at 2.4 Å resolution (Fig. 1A). Both L-arginine and glycerol bound to the active site pocket, and the recognition and orientation of L-arginine at this site were similar to those of *S. cerevisiae* ArgRS [27,28] and the *hArgRS*-L-canavanine complex (Fig. 1B). The structural analysis revealed that the nitrogen atom of L-arginine interacts directly with Ser128 and Asn130 and indirectly with the side chain of Glu263 through Wat6 (Fig. 1C). The L-arginine carboxyl group forms hydrogen bonds with Asn130, His139, and

Gln340. In addition, the negatively charged residues, Asp125 and Asp316, interact with the substrate's guanidino group, as well as Tyr312.

Glycerol bound to the active site pocket located between the C-terminus of the  $\beta$ 11 strand and the N-terminus of the  $\alpha$ 5 helix (Fig. 1A and B). It interacted with the side chain of Ser142 and the main chains of Asp337 (Fig. 1C). Notably, glycerol was situated in the ATP-analog binding region corresponding to that of *P. horikoshii* ArgRS [29]. The interaction between glycerol and Ser142 mimics the hydrogen bond formed between the 3'-carbon of an ATP-analog pentose sugar and Asn141 via a water molecule in *P. horikoshii* ArgRS. The interaction of Asp337 with glycerol also mimics the interaction between the 2'-carbon of an ATP-analog pentose sugar and the main chain of Gly384. Although these results

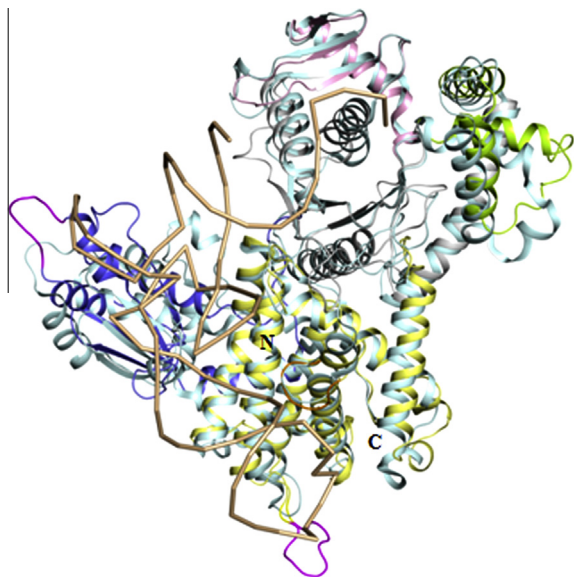


**Fig. 3.** A structural superimposition of *hArgRS* and *S. cerevisiae* ArgRS bound to tRNA<sup>Arg</sup> with L-arginine [28]. The *hArgRS* domains are colored as described for Fig. 1A. *S. cerevisiae* ArgRS is shown as a pale cyan ribbon model. The structural inserted regions and the  $\Omega$  loop of *hArgRS* are indicated in magenta and orange, respectively.

indicate that *hArgRS* interacts with ATP in this region, the binding pocket is too small. Consequently, conformational changes of the loop between the  $\beta 5$  strand and the  $\alpha 5$  helix, and the N-terminus of the  $\alpha 5$  helix containing the 'HIGH' motif, are required for ATP binding. The derived size of the ATP binding pocket in the presence of arginine gives a molecular basis as to why tRNA is required for arginine activation [28].

#### 3.4. Comparisons of the L-canavanine and L-arginine binding sites

The interactions between the active site of *hArgRS* and L-canavanine were similar to those between the active site and L-arginine. However, the interaction between Tyr312 and the oxygen of the oxyguanidino group differed between these complexes (Fig. 1D). Tyr312 pulls the oxyguanidino group, twisting L-canavanine, which is slightly longer than L-arginine, and causing Asp316 to interact with the oxyguanidino group (Fig. 1D and E). Tyr312 is essential for the stable binding of L-canavanine. Compared with *hArgRS*-L-canavanine, the positions of two residues, namely Asp337 and Asp316, were shifted in *hArgRS*-L-arginine (Fig. 1E). In *hArgRS*-L-canavanine, Asp337 interacts with the carboxyl group of the substrate via Wat50. This residue is not conserved among other organisms and the interaction was not observed in *hArgRS*-L-arginine or *S. cerevisiae* ArgRS-L-arginine. This interaction may stabilize binding of the carboxyl group of L-canavanine to Asn130, His139, and Gln340 of *hArgRS*.

#### 3.5. Structural conformational changes

Previous reports of the structure of ArgRS discussed the conformational changes that occur upon binding to tRNA<sup>Arg</sup> with and without L-arginine, as well as an ATP analog [27–29]. Here, to provide insight into the conformational changes that occur during recognition of L-canavanine and L-arginine in the absence of tRNA<sup>Arg</sup>, the structures of the apo, L-canavanine-complexed, and L-arginine-complexed forms of *hArgRS* were compared (Fig. 2A–E). The loops in the Nd between the  $\alpha 2$  helix and the  $\beta 1$  strand, and between the  $\alpha 2$  and  $\alpha 3$  helices, were disordered in the apo struc-

ture (Fig. 2D). The analysis revealed that, in the absence of the substrate, the active site pocket is maintained in an open state by Asn130, Glu263, and Tyr312 (Fig. 2A). By interacting with the side chain of Gln172 in the  $\alpha 6$  helix of Ins1 via Wat25, Tyr312 is positioned close to Ins1, and Gln172 forms two hydrogen bonds with the side chains of Asn130 and Tyr201. The side-chain carboxyl group of Glu263 also interacts with the main chain of Trp169. These interactions generate the open substrate-accessible pocket. The active site residues, Asn130, Tyr312, Asp316, and Gln340, shift to recognize the substrate (Fig. 2B, C and E). In particular, Asn130, Tyr312, and Gln340 are associated with the closed form of the active site pocket, as well as several other residues. Asn130 shifts to form hydrogen bonds with the carboxyl and amino groups of the substrate, and Gln340 shifts to interact with its carboxyl group. Tyr312 and Asp316 move towards the oxyguanidino group of L-canavanine and the guanidinium group of L-arginine (Fig. 2B and C). In addition, Glu263 shifts to interact with the side chain of Ser315. Shifting of Glu263 and Tyr312 are essential for creating the closed form of the active site pocket and preventing access by another substrate. Therefore, shifting of the active site and surrounding residues, especially Asn130 and Tyr312, are required for formation of the active site pocket and substrate recognition.

Shifting of Tyr312 and Glu263 forms a cavity that is accessed by the acceptor arm of tRNA<sup>Arg</sup> (Fig. 2B and C). Comparison of the structures of tRNA<sup>Arg</sup>-bound ArgRS from *S. cerevisiae* in the presence and absence of L-arginine revealed that Tyr347 is essential for the correct localization of the CCA end of tRNA<sup>Arg</sup> [28]. In the absence of the substrate, this residue prevents proper positioning of the CCA end of tRNA<sup>Arg</sup> via interaction with the main chain of Trp192, and in the presence of substrate, it generates the conformational change necessary to stabilize the CCA end. By contrast, the structural analysis described here revealed that, in the absence of substrate, a tRNA<sup>Arg</sup> acceptor arm-accessible cavity is not generated in *hArgRS* though indirect interactions of Tyr312 with Glu172 and Asn130 via Wat25, and interaction of the side chain of Glu263 with the main chain of Trp169 (Fig. 2A). In the presence of L-arginine- or L-canavanine-, the shifted Tyr312 and Glu263 residues of *hArgRS*, which interact with the substrate and Ser315, respectively, form the tRNA<sup>Arg</sup> acceptor arm-accessible cavity (Fig. 2B and C). Glu263 in *hArgRS* corresponds to Glu294 in *S. cerevisiae* ArgRS [28], which is an important residue for locking the 3'-OH group of the Ade76 residue of tRNA<sup>Arg</sup> via a hydrogen bond. These results suggest that, like L-arginine, binding of L-canavanine to the active site of *hArgRS* gives rise to the formation of a pocket for binding of the tRNA<sup>Arg</sup> acceptor arm.

#### 3.6. Comparisons with other structures

Although the sequence identities of ArgRSs from *H. sapiens* and other organisms (*S. cerevisiae*, *T. thermophilus*, and *P. horikoshii*) are considerably low (<25.9%), the overall structures are similar (Fig. 4 and Supplementary Fig. 1). The root mean square deviation (RMSD) of the overall structures of *hArgRS* and *S. cerevisiae* ArgRS was 1.86 Å (calculated with 383 C $\alpha$  atoms). The catalytic and Cd domains of these proteins are also similar, with RMSDs of 0.75 and 0.83 Å (calculated with 111 and 123 C $\alpha$  atoms), respectively. However, the Nd, Ins1, and Ins2 are markedly different with RMSDs of 7.09, 3.89, and 10.48 Å (calculated with 82, 38, and 30 C $\alpha$  atoms), respectively (Supplementary Fig. 1). In the catalytic domain, the substrate recognition sites and the 'HIGH' motif, in which Ile is replaced with Val, are conserved, while the 'KMSKS' motif, which is located within the loop between Ins2 and Cd, is not conserved and is structurally flexible (Figs. 1A and 4).

The long loop in the Nd of *hArgRS* was not observed in the structures of the ArgRSs from *P. horikoshii*, *T. thermophilus*, or *S. cerevisiae* (Supplementary Fig. 1). This loop contains an insertion



**Fig. 4.** Multiple sequence alignment of ArgRSs from *H. sapiens* (H\_sa), *S. cerevisiae* (S\_ce), *T. thermophilus* (T\_th), and *P. horikoshii* (P\_ho). The alignment was generated using ESPrit [31]. Residues conserved across all four species are shaded red and residues conserved across three species are shown in red text. The secondary structure of hArgRS is shown above the alignment and is colored as in Fig. 1A.

(Lys54–Val60) between the  $\alpha 2$  and  $\alpha 3$  helices (Fig. 3). Based on structural superposition of hArgRS and *S. cerevisiae* ArgRS bound to tRNA<sup>Arg</sup> [28], the region is predicted to be involved in binding and stabilization of the T $\psi$ C loop of tRNA<sup>Arg</sup> and may also stabilize tRNA<sup>Arg</sup> binding (Fig. 3). Furthermore, hArgRS has a long tRNA<sup>Arg</sup> anticodon-binding loop between the  $\alpha 19$  and  $\alpha 20$  helices in the Cd; residues in this region that are involved in the recognition and conformation of the tRNA<sup>Arg</sup> anticodon loop (Tyr464, Arg468, Arg474, Tyr540, Tyr544 and Met588) are highly conserved. Trp569, which forms a stacking interaction between Ino34 and Cyt35 of the tRNA<sup>Arg</sup> anticodon in *S. cerevisiae* ArgRS, is replaced with Tyr544 in hArgRS. The long anticodon tRNA<sup>Arg</sup>-binding loop contains a structurally inserted region (Lys548–Leu556) that is thought to aid the interaction with and stabilization of the conformation of the tRNA<sup>Arg</sup> anticodon loop (Fig. 3). The characteristic  $\Omega$  loop, which is related to the correct location of the anticodon through interaction with the major groove of the anticodon stem, was also identified in hArgRS (Fig. 3). A protruding region comprising six residues (Asp453–Thr458) between the  $\alpha 15$  and  $\alpha 16$  helices is not conserved; however, Gly456, which corresponds to

Gly483 in *S. cerevisiae* ArgRS that has a functional role in cell growth, is conserved [30]. Gly483 plays a vital role for positioning of the major groove of the anticodon stem because its mutation to any other residue interferes with tRNA<sup>Arg</sup> positioning [28].

#### Acknowledgements

We thank the staff of beamline 4A at the Pohang Accelerator Laboratory and beamline BL1A at the Photon Factory for technical support (2012G189). We are also grateful to the staff at the Korean Basic Science Institute (Daejeon, Korea) for the use of a mosquito crystallization robot and the Rigaku MicroMax-007HF X-ray generator. This work was supported by grants from the National Research Foundation of Korea (2013-044795).

#### Appendix A. Supplementary data

Supplementary data associated with this article can be found, in the online version, at <http://dx.doi.org/10.1016/j.febslet.2014.05.027>.

## References

- [1] Ibba, M. and Soll, D. (2000) Aminoacyl-tRNA synthesis. *Annu. Rev. Biochem.* 69, 617–650.
- [2] Eriani, G., Delarue, M., Poch, O., Gangloff, J. and Moras, D. (1990) Partition of tRNA synthetases into two classes based on mutually exclusive sets of sequence motifs. *Nature* 347, 203–206.
- [3] Ferber, S. and Ciechanover, A. (1987) Role of arginine-tRNA in protein degradation by the ubiquitin pathway. *Nature* 326, 808–811.
- [4] Yang, F., Xia, X., Lei, H.Y. and Wang, E.D. (2010) Hemin binds to human cytoplasmic arginyl-tRNA synthetase and inhibits its catalytic activity. *J. Biol. Chem.* 285, 39437–39446.
- [5] Deutscher, M.P. and Ni, R.C. (1982) Purification of a low molecular weight form of rat liver arginyl-tRNA synthetase. *J. Biol. Chem.* 257, 6003–6006.
- [6] Vellekamp, G. and Deutscher, M.P. (1987) A basic NH<sub>2</sub>-terminal extension of rat liver arginyl-tRNA synthetase required for its association with high molecular weight complexes. *J. Biol. Chem.* 262, 9927–9930.
- [7] Sivaram, P. and Deutscher, M.P. (1990) Existence of two forms of rat liver arginyl-tRNA synthetase suggests channeling of aminoacyl-tRNA for protein synthesis. *Proc. Natl. Acad. Sci. U.S.A.* 87, 3665–3669.
- [8] Lazard, M., Agou, F., Kerjan, P. and Mirande, M. (2000) The tRNA-dependent activation of arginine by arginyl-tRNA synthetase requires inter-domain communication. *J. Mol. Biol.* 302, 991–1004.
- [9] Zheng, Y.G., Wei, H., Ling, C., Xu, M.G. and Wang, E.D. (2006) Two forms of human cytoplasmic arginyl-tRNA synthetase produced from two translation initiations by a single mRNA. *Biochemistry* 45, 1338–1344.
- [10] Mehler, A.H. and Mitra, S.K. (1967) The activation of arginyl transfer ribonucleic acid synthetase by transfer ribonucleic acid. *J. Biol. Chem.* 242, 5495–5499.
- [11] Papas, T.S. and Peterkofsky, A. (1972) A random sequential mechanism for arginyl transfer ribonucleic acid synthetase of *Escherichia coli*. *Biochemistry* 11, 4602–4608.
- [12] Kern, D. and Lapointe, J. (1980) Catalytic mechanism of glutamyl-tRNA synthetase from *Escherichia coli*. Reaction pathway in the aminoacylation of tRNA<sup>Glu</sup>. *Biochemistry* 19, 3060–3068.
- [13] Guigou, L., Shalak, V. and Mirande, M. (2004) The tRNA-interacting factor p43 associates with mammalian arginyl-tRNA synthetase but does not modify its tRNA aminoacylation properties. *Biochemistry* 43, 4592–4600.
- [14] Ling, C., Yao, Y.N., Zheng, Y.G., Wei, H., Wang, L., Wu, X.F. and Wang, E.D. (2005) The C-terminal appended domain of human cytosolic leucyl-tRNA synthetase is indispensable in its interaction with arginyl-tRNA synthetase in the multi-tRNA synthetase complex. *J. Biol. Chem.* 280, 34755–34763.
- [15] Lee, S.W., Cho, B.H., Park, S.G. and Kim, S. (2004) Aminoacyl-tRNA synthetase complexes: beyond translation. *J. Cell Sci.* 117, 3725–3734.
- [16] Tasaki, T. and Kwon, Y.T. (2007) The mammalian N-end rule pathway: new insights into its components and physiological roles. *Trends Biochem. Sci.* 32, 520–528.
- [17] Kitagawa, M. and Tomiyama, T. (1926) A new amino-compound in the jack bean and a corresponding new ferment. *J. Biochem.* 11, 256–271.
- [18] Rosenthal, G.A., Reichhart, J.M. and Hoffmann, J.A. (1989) L-Canavanine incorporation into vitellogenin and macromolecular conformation. *J. Biol. Chem.* 264, 13693–13696.
- [19] Bence, A.K. and Crooks, P.A. (2003) The mechanism of L-canavanine cytotoxicity: arginyl tRNA synthetase as a novel target for anticancer drug discovery. *J. Enzyme Inhib. Med. Chem.* 18, 383–394.
- [20] Swaffar, D.S., Ang, C.Y., Desai, P.B. and Rosenthal, G.A. (1994) Inhibition of the growth of human pancreatic cancer cells by the arginine antimetabolite L-canavanine. *Cancer Res.* 54, 6045–6048.
- [21] Rosenthal, G.A. (1977) The biological effects and mode of action of L-canavanine, a structural analogue of L-arginine. *Q. Rev. Biol.* 52, 155–178.
- [22] Otwinowski, Z. and Minor, W. (1997) Processing of X-ray diffraction data collected in oscillation mode. *Methods Enzymol.* 276, 307–326.
- [23] Adams, P.D. et al. (2010) PHENIX: a comprehensive Python-based system for macromolecular structure solution. *Acta Crystallogr. D Biol. Crystallogr.* 66, 213–221.
- [24] Emsley, P., Lohkamp, B., Scott, W.G. and Cowtan, K. (2010) Features and development of Coot. *Acta Crystallogr. D Biol. Crystallogr.* 66, 486–501.
- [25] Chen, V.B. et al. (2010) MolProbity: all-atom structure validation for macromolecular crystallography. *Acta Crystallogr. D Biol. Crystallogr.* 66, 12–21.
- [26] Krissinel, E. and Henrick, K. (2007) Inference of macromolecular assemblies from crystalline state. *J. Mol. Biol.* 372, 774–797.
- [27] Cavarelli, J., Delagoutte, B., Eriani, G., Gangloff, J. and Moras, D. (1998) L-Arginine recognition by yeast arginyl-tRNA synthetase. *EMBO J.* 17, 5438–5448.
- [28] Delagoutte, B., Moras, D. and Cavarelli, J. (2000) tRNA aminoacylation by arginyl-tRNA synthetase: induced conformations during substrates binding. *EMBO J.* 19, 5599–5610.
- [29] Konno, M., Sumida, T., Uchikawa, E., Mori, Y., Yanagisawa, T., Sekine, S. and Yokoyama, S. (2009) Modeling of tRNA-assisted mechanism of Arg activation based on a structure of Arg-tRNA synthetase, tRNA, and an ATP analog (ANP). *FEBS J.* 276, 4763–4779.
- [30] Geslain, R., Martin, F., Delagoutte, B., Cavarelli, J., Gangloff, J. and Eriani, G. (2000) In vivo selection of lethal mutations reveals two functional domains in arginyl-tRNA synthetase. *RNA* 6, 434–448.
- [31] Brown, E.N., Friemann, R., Karlsson, A., Parales, J.V., Couture, M.M., Eltis, L.D. and Ramaswamy, S. (2008) Determining Rieske cluster reduction potentials. *J. Biol. Inorg. Chem.* 13, 1301–1313.